MATHEMATICAL BIOSCIENCES
AND ENGINEERING
Volume ?, Number 0?, ? 2004

http://math.asu.edu/~mbe/

pp. 1–??

MODELING THE CONTROL OF THE HUMAN CARDIOVASCULAR-RESPIRATORY SYSTEM: AN OPTIMAL CONTROL APPROACH WITH APPLICATION TO THE TRANSITION TO NON-REM SLEEP

Susanne Timischl-Teschl

Fachhochschule Technikum Wien
Hoechstaedtplatz 5, 1200 Wien, Austria

Jerry J. Batzel

Special Research Center "Optimization and Control, University of Graz
Heinrichstraße 22, A-8010 Graz, Austria.

Franz Kappel

Institute for Mathematics and Scientific Computing
Heinrichstraße 36, A-8010 Graz, Austria.

Abstract. In this paper we discuss a model of the human cardiovascular-respiratory control system. The mechanisms which control the ventilation rate $\dot{V}_A$ are fairly well understood and mathematical equations have been devised to describe this control. The cardiovascular control system, on the other hand, involves a complex set of interrelationships between heart rate, blood pressure, cardiac output, and blood vessel resistance. At the current time no set of equations fully describes these control relationships. In this paper we will approach the modeling of the control system by viewing it as an optimal control problem. The derived control will act to stabilize the system by moving the system from a perturbed state to a final steady state in an optimal way. This is a reasonable approach based on mathematical considerations as well as being further motivated by the observation that many physiologists cite optimization as a potential influence in the evolution of biological systems (see, e.g., Kenner [1] or Swan [2]). We present a model developed in Timischl [3] and as an application of this model we will consider the transition from the quiet awake state to stage 4 (NREM) sleep. The model can provide a basis for developing information on steady state relations and also to study the nature of the controller and key controlling influences. The model provides an approach for studying the complex physiological control mechanisms of the cardiovascular system and possible paths of interaction between the cardiovascular and respiratory control systems. The influence of optimality on physiological control systems can also be examined.

2000 *Mathematics Subject Classification.* 92C30, 49J15.

Key words and phrases. Respiratory system, Cardiovascular System, Optimal control, Modeling.

1. **Introduction.** Control mechanisms are integral to the function of the cardiovascular and respiratory systems. The respiratory system functions to exchange metabolic byproducts, such as CO_2, for O_2, which is necessary for metabolism. Gas exchange is accomplished solely by passive diffusion across the blood/gas barrier between capillaries and alveoli. Hence, it is essential to maintain a significant pressure gradient across this barrier under varying load conditions. This is accomplished by varying the ventilation rate $\dot{V}_A$ which is the rate at which fresh air is introduced into the alveoli. As a result of this exchange the blood leaving the lungs via the pulmonary veins has a high O_2 and a low CO_2 concentration. The reverse exchange occurs in the tissues where metabolic activity utilizes O_2 and produces as a byproduct CO_2.

The human respiratory control system varies the ventilation rate in response to the levels of CO_2 and O_2 in the body (via partial pressures $P_{a_{CO_2}}$ and $P_{a_{O_2}}$). This is referred to as the chemical control system (to distinguish it from voluntary control). The chemical control system involves two sensory sites which monitor the blood gas levels producing a negative feedback control loop. This system plays the major role in ventilation control during periods of unconsciousness, sleep, and when voluntary control is absent. The control mechanism acts to maintain the blood levels of these gases within very narrow limits.

The cardiovascular system manages blood flow to various regions of the body and its function depends on a large number of factors including cardiac output, blood pressure, cross-section of arteries and partial pressures of CO_2 and O_2 in the blood. Blood flow is regulated by both global mechanisms of control and by local control mechanisms in each region. The control mechanisms which stabilize the system are quite complicated and not fully understood. Arterial blood pressure P_{as} is controlled via the baroreceptor negative feedback loop. This mechanism influences global control (there is also local control) of resistance in the blood vessels as well as well as heart rate H and stroke volume V_{str} all of which are important factors impacting cardiac output Q. Because of the complexity of interaction of the various control loops we will consider a control derived from principles of optimal control theory. For further details about the physiology of the cardiovascular control system see, e.g., Rowell [4].

The cardiovascular system is linked to the respiratory system via the blood flow through the lungs and tissues. Oxygen transported to the tissues depends on cardiac output Q (and blood flow F) to the pulmonary and systemic circuits. Q is adjusted by varying H and V_{str}.

The respiratory quantities CO_2 and O_2 affect the cardiovascular system in a number of ways. This model includes the effect of the venous concentration of O_2 on the resistance of the systemic blood vessels. Furthermore, research indicates that $P_{a_{CO_2}}$ and $P_{a_{O_2}}$ affect cardiac output and contractility as well (see, e.g., Richardson *et al.* [5]). These effects have not been considered

in this model. There is some synchronization of ventilatory and heart rate frequencies as well.

As alluded to above, in this analysis, we will model the complex interactions in the cardiovascular-respiratory control system using results from optimal control theory. The cardiovascular and respiratory control will be represented by a linear feedback control which minimizes a quadratic cost functional. Motivation for the optimal approach is given in Section 3. The state equations draw extensively on the work of Khoo *et al.* [6], Grodins and coworkers [7, 8, 9], and Kappel and coworkers [10, 11, 12].

This modeling approach was previously used by Timischl [3] to study transition from rest to exercise under a constant ergometric workload and the role of pulmonary circulatory resistance during exercise. The model can be applied to study a number of cardiovascular parameters and quantities which vary in ways not fully worked out or adequately measured. The model can be used to examine cardiac output, contractility, and systemic and pulmonary vascular resistance changes during transition in functional states and to explore connections between these and other quantities in clinical conditions such as congestive heart failure.

2. **The model.** The model describing the cardiovascular-respiratory system is given by the following set of 13 differential equations,

$$\begin{aligned}
V_{A_{CO_2}}\dot{P}_{a_{CO_2}}(t) &= 863F_p(t)(C_{v_{CO_2}}(t) - C_{a_{CO_2}}(t)) \\
&\quad + \dot{V}_A(t)(P_{I_{CO_2}} - P_{a_{CO_2}}(t)), \qquad (1)\\
V_{A_{O_2}}\dot{P}_{a_{O_2}}(t) &= 863F_p(t)(C_{v_{O_2}}(t) - C_{a_{O_2}}(t)) \\
&\quad + \dot{V}_A(t)(P_{I_{O_2}} - P_{a_{O_2}}(t)), \qquad (2)\\
V_{T_{CO_2}}\dot{C}_{v_{CO_2}}(t) &= MR_{CO_2} + F_s(t)(C_{a_{CO_2}}(t) - C_{v_{CO_2}}(t)), \qquad (3)\\
V_{T_{O_2}}\dot{C}_{v_{O_2}}(t) &= -MR_{O_2} + F_s(t)(C_{a_{O_2}}(t) - C_{v_{O_2}}(t)), \qquad (4)\\
c_{as}\dot{P}_{as}(t) &= Q_l(t) - F_s(t), \qquad (5)\\
c_{vs}\dot{P}_{vs}(t) &= F_s(t) - Q_r(t), \qquad (6)\\
c_{vp}\dot{P}_{vp}(t) &= F_p(t) - Q_l(t), \qquad (7)\\
\dot{S}_l(t) &= \sigma_l(t), \qquad (8)\\
\dot{S}_r(t) &= \sigma_r(t), \qquad (9)\\
\dot{\sigma}_l(t) &= -\gamma_l\sigma_l(t) - \alpha_l S_l(t) + \beta_l H(t), \qquad (10)\\
\dot{\sigma}_r(t) &= -\gamma_r\sigma_r(t) - \alpha_r S_r(t) + \beta_r H(t), \qquad (11)\\
\dot{H}(t) &= u_1(t), \qquad (12)\\
\ddot{V}_A(t) &= u_2(t). \qquad (13)
\end{aligned}$$

This combined model was developed and studied in Timischl [3]. A complete list of symbols is given in Tables 1 and 2.

TABLE 1. Respiratory symbols

Symbol	Meaning	unit
$C_{a_{CO_2}}$	concentration of bound and dissolved CO_2 in arterial blood	$\mathrm{l}_{\mathrm{STPD}} \cdot \mathrm{l}^{-1}$
$C_{a_{O_2}}$	concentration of bound and dissolved O_2 in arterial blood	$\mathrm{l}_{\mathrm{STPD}} \cdot \mathrm{l}^{-1}$
$C_{v_{CO_2}}$	concentration of bound and dissolved CO_2 in mixed venous blood entering the lungs	$\mathrm{l}_{\mathrm{STPD}} \cdot \mathrm{l}^{-1}$
$C_{v_{O_2}}$	concentration of bound and dissolved O_2 in the mixed venous blood entering the lungs	$\mathrm{l}_{\mathrm{STPD}} \cdot \mathrm{l}^{-1}$
MR_{CO_2}	metabolic CO_2 production rate	$\mathrm{l}_{\mathrm{STPD}} \cdot \mathrm{min}^{-1}$
MR_{O_2}	metabolic O_2 consumption rate	$\mathrm{l}_{\mathrm{STPD}} \cdot \mathrm{min}^{-1}$
$P_{a_{CO_2}}$	partial pressure of CO_2 in arterial blood	mmHg
$P_{a_{O_2}}$	partial pressure of O_2 in arterial blood	mmHg
$P_{v_{CO_2}}$	partial pressure of CO_2 in mixed venous blood	mmHg
$P_{v_{O_2}}$	partial pressure of O_2 in mixed venous blood	mmHg
P_I	partial pressure of inspired gas	mmHg
B	brain compartment	-
u_2	control function, $u_2 = \ddot{V}_A$	$\mathrm{l}_{\mathrm{BTPS}} \cdot \mathrm{min}^{-2}$
$\dot{V}_A$	alveolar ventilation	$\mathrm{l}_{\mathrm{BTPS}} \cdot \mathrm{min}^{-1}$
$\ddot{V}_A$	time derivative of alveolar ventilation	$\mathrm{l}_{\mathrm{BTPS}} \cdot \mathrm{min}^{-2}$
$V_{A_{CO_2}}$	effective CO_2 storage volume of the lung compartment	$\mathrm{l}_{\mathrm{BTPS}}$
$V_{A_{O_2}}$	effective O_2 storage volume of the lung compartment	$\mathrm{l}_{\mathrm{BTPS}}$
$V_{T_{CO_2}}$	effective tissue storage volume for CO_2	l
$V_{T_{O_2}}$	effective tissue storage volume for O_2	l
I_p, I_c	cutoff thresholds	mmHg

The respiratory component is defined by equations (1) to (4) and is based on equations given in Khoo *et al.* [6]. The respiratory system is modeled using two compartments: a lung compartment and a general tissue compartment (see Figure 1). The lung compartment equations (1) and (2) represent mass balance equations for CO_2 and O_2, respectively. Equations (3) and (4) are the state equations, respectively, for CO_2 and O_2 in the tissue compartment. The model incorporates alveolar minute ventilation (effective ventilation) and thus does not reflect breath to breath effects or the modulation of rate and depth of breathing which can influence stability (see Batzel and Tran [13, 14]). For the purposes of this general flow model, the overall minute ventilation is sufficient.

The lung compartment alveolar blood gas levels are assumed to be equilibrated with the arterial levels and similarly the tissue compartment blood concentrations are assumed to be equilibrated with the venous concentrations. Other assumptions are given in the appendix. For present purposes we do not include delays in the model.

The cardiovascular model equations are based on the work of Grodins *et al.* [7, 8, 9] and Kappel *et al.* [10, 15, 11] and Peer [12] and is described by equations (5) to (11). The model consists of two circuits (systemic and pulmonary) which are arranged in series, and two pumps (left and right ventricle). Figure 1 gives a block diagram for the model. The complex of arteries and veins, arterioles, and capillary networks of each circuit is

TABLE 2. Cardiovascular symbols

Symbol	Meaning	Unit
α_l	coefficient of S_l in the differential equation for σ_l	min^{-2}
α_r	coefficient of S_r in the differential equation for σ_r	min^{-2}
A_{pesk}	$R_s = A_{\text{pesk}} C_{v_{O_2}}$	$\text{mmHg} \cdot \text{min} \cdot \text{l}^{-1}$
β_l	coefficient of H in the differential equation for σ_l	$\text{mmHg} \cdot \text{min}^{-1}$
β_r	coefficient of H in the differential equation for σ_r	$\text{mmHg} \cdot \text{min}^{-1}$
c_{as}	compliance of the arterial part of the systemic circuit	$\text{l} \cdot \text{mmHg}^{-1}$
c_{ap}	compliance of the arterial part of the pulmonary circuit	$\text{l} \cdot \text{mmHg}^{-1}$
c_{vs}	compliance of the venous part of the systemic circuit	$\text{l} \cdot \text{mmHg}^{-1}$
c_{vp}	compliance of the venous part of the pulmonary circuit	$\text{l} \cdot \text{mmHg}^{-1}$
F_p	blood flow perfusing the lung compartment	$\text{l} \cdot \text{min}^{-1}$
F_s	blood flow perfusing the tissue compartment	$\text{l} \cdot \text{min}^{-1}$
H	heart rate	min^{-1}
γ_l	coefficient of σ_l in the differential equation for σ_l	min^{-1}
γ_r	coefficient of σ_r in the differential equation for σ_r	min^{-1}
P_{as}	mean blood pressure in arterial region: systemic circuit	mmHg
P_{ap}	mean blood pressure in arterial region: pulmonary circuit	mmHg
P_{vs}	mean blood pressure in venous region: systemic circuit	mmHg
P_{vp}	mean blood pressure in venous region: pulmonary circuit	mmHg
Q_l	left cardiac output	$\text{l} \cdot \text{min}^{-1}$
Q_r	right cardiac output	$\text{l} \cdot \text{min}^{-1}$
R_p	resistance in the peripheral region of the pulmonary circuit	$\text{mmHg} \cdot \text{min} \cdot \text{l}^{-1}$
R_s	peripheral resistance in the systemic circuit	$\text{mmHg} \cdot \text{min} \cdot \text{l}^{-1}$
S_l	contractility of the left ventricle	mmHg
S_r	contractility of the right ventricle	mmHg
σ_l	derivative of S_l	$\text{mmHg} \cdot \text{min}^{-1}$
σ_r	derivative of S_r	$\text{mmHg} \cdot \text{min}^{-1}$
u_1	control function, $u_1 = \dot{H}$	min^{-2}
$V_{str,l}$	stroke volume of the left ventricle	l
$V_{str,r}$	stroke volume of the right ventricle	l
V_0	total blood volume	l

lumped into three components: a single elastic artery, a single elastic vein, and a single resistance vessel. We assume a unidirectional non-pulsatile blood flow through the heart. Hence, blood flow and blood pressure have to be interpreted as mean values over the length of a pulse. Other important assumptions are provided in the appendix. Equations (5) and (6) are the blood mass balance equations in the systemic artery and vein components, respectively. Equation (7) refers to the mass balance equation in the pulmonary vein component. Utilizing the assumption of a fixed blood volume V_0, the equation for the pulmonary artery can be described by the algebraic relation

$$P_{ap}(t) = \frac{1}{c_{ap}}(V_0 - c_{as}P_{as}(t) - c_{vs}P_{vs}(t) - c_{vp}P_{vp}(t)). \tag{14}$$

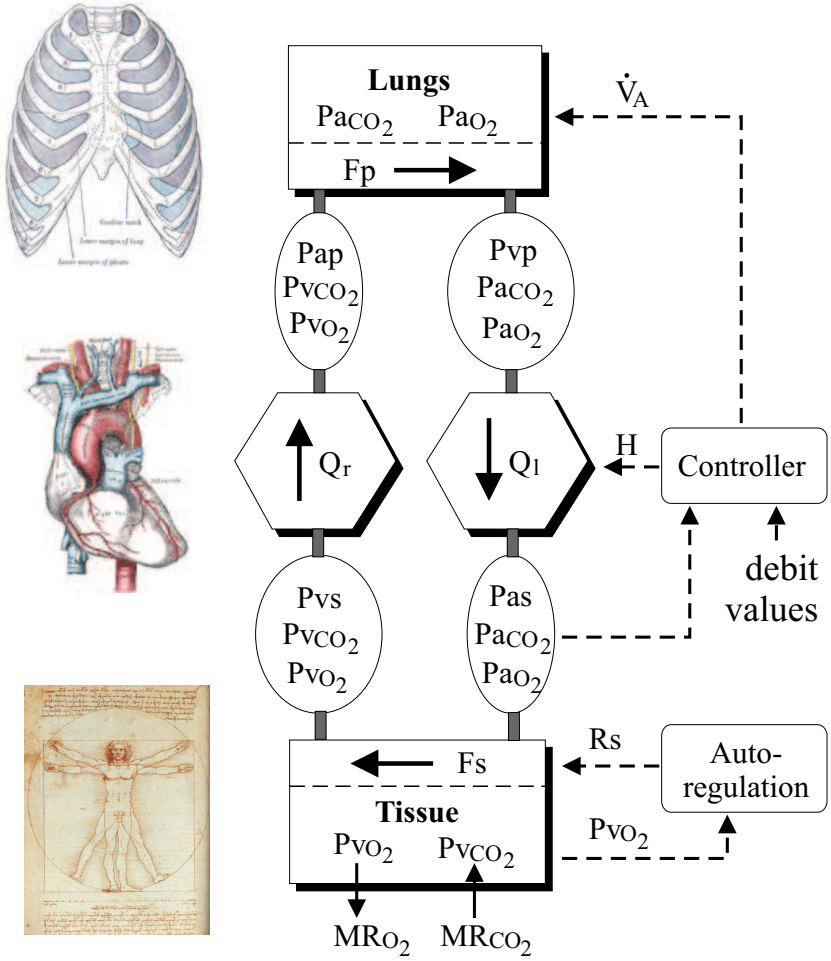

FIGURE 1. Model block diagram

In equations (5) through (7) the dependencies of blood flow F on blood pressure are given by what is essentially Ohm's law

$$F_s(t) = \frac{P_{as}(t) - P_{vs}(t)}{R_s(t)}, \tag{15}$$

$$F_p(t) = \frac{P_{ap}(t) - P_{vp}(t)}{R_p}, \tag{16}$$

where P_a is arterial blood pressure, P_v is venous pressure, and R is vascular resistance. Cardiac output Q is defined as the mean blood flow over the length of a pulse,

$$Q(t) = H(t)V_{str}(t), \tag{17}$$

where H is the heart rate and V_{str} is the stroke volume (here we have omitted the subindices, since analogous relations hold for the right and left ventricle).

A relationship between stroke volume and blood pressure is given in Kappel and Peer [10]. It incorporates the Frank-Starling law and essentially reflects the relation

$$V_{str}(t) = S(t)\frac{cP_v(t)}{P_a(t)}. \tag{18}$$

Here S denotes the contractility, P_v is the venous filling pressure, P_a is the arterial blood pressure opposing the ejection of blood. and c denotes the compliance of the relaxed ventricle. Equations (8) through (11) describe the observation that the contractility S_l respectively S_r increases if heart rate increases (Bowditch effect). This is modeled via a second order differential equation. For details see Kappel and Peer [10].

Finally, equations (12) and (13) define the variation of heart rate $\dot{H}$ and the variation of ventilation rate $\ddot{V}_A$ as control variables. The functions $u_1(t)$ and $u_2(t)$ will be determined by an optimality criterion (see Section 3). Note that $\dot{V}_A(t)$ in the state equations for the lung compartment (1) and (2) represents effective ventilation and reflects net ventilation after respiratory dead space effects are taken into account.

The respiratory and cardiovascular submodels are linked in the following ways. The respiratory mass balance equations include expressions for the blood flows F_s and F_p. The respiratory system in turn influences the cardiovascular system via the local metabolic autoregulation. This is modeled by the assumption that systemic resistance R_s depends on venous oxygen concentration $C_{v_{O_2}}$,

$$R_s(t) = A_{pesk}C_{v_{O_2}}(t), \tag{19}$$

where A_{pesk} is a parameter. Some tissues respond to $C_{v_{CO_2}}$ as well but we assume the main contributor to system resistance is reflected in the above equation. This relationship was originally introduced by Peskin [16]. It is based on a model for autoregulation first developed by Huntsman *et al.* [17]. Relationship (19) was also used in Kappel and Peer [10] and related papers. This equation expresses an important local control mechanism for varying vascular resistance. We consider global changes in R_s in a later section (Section 6). Furthermore, the influence of heart rate H and ventilation rate $\dot{V}_A$ on the system is implemented through the control functions u_1 and u_2. The states P_{as}, $P_{a_{CO_2}}$, and $P_{a_{O_2}}$, affect the dynamical behavior through the cost functional. We note that blood gas partial pressures and concentrations are interchangeable according to the dissociation formulas (see the Appendix). We use concentrations in some state equations to simplify the form of the equations.

3. **The control mechanisms.** Given the complex (and not fully elucidated) interaction of the various control loops, we have incorporated a unified stabilizing control that is derived from optimal control theory. We will design the cardiovascular and the respiratory control systems to transfer the system from a steady state "initial disturbance" to the steady state "final

equilibrium" in an optimal way to be defined below. Thus the control will be a stabilizing control returning the system to equilibrium and this mathematical formulation of the control is incorporated into the model for this purpose. This approach can provide information on the nature of the physiological control process as well as to identify and study key controlling and controlled quantities.

We note that such an approach in designing a stabilizing control is reasonable given that many physiologists consider optimization as a potential basic influence in the evolution of biological systems (see, e.g., Kenner [1] or Swan [2]). For example, minimum energy usage is a reasonable design requirement for a control system. The degree and manner in which optimization is reflected in design is an open question and thus the approach taken here follows primarily from mathematical considerations to develop a stabilizing control.

It is the task of the baroreceptor loop to stabilize the arterial systemic pressure P_{as} around an equilibrium operating point denoted by P_{as}^f for final or target operating point. Further, it appears that a main goal of respiratory control is to keep CO_2 partial pressure as close as possible to an equilibrium value denoted by $P_{a_{CO_2}}^f$ and, to a lesser extent, control O_2 to the equilibrium $P_{a_{O_2}}^f$. We assume that the variables P_{as}, $P_{a_{CO_2}}$, and $P_{a_{O_2}}$, are returned to their stable equilibrium values as efficiently as possible but with the constraint that the controlling quantities, heart rate H and alveolar ventilation $\dot{V}_A$, must not be altered too fast, and that variations in these quantities are not too extreme. This constraint corresponds to the requirement that the control effort should be as small as possible as well as physiologically reasonable. In this way, the feedback control can be referred to not only as a stabilizing but also as an optimizing control.

When an initial disturbance occurs, H and $\dot{V}_A$ are adjusted so that the mean arterial blood pressure P_{as}, arterial partial pressures of carbon dioxide $P_{a_{CO_2}}$, and arterial oxygen $P_{a_{O_2}}$ (as well as the system as a whole) are stabilized to their final steady state operating points. The final operating point or final steady state for a given physiological condition is defined by the choice of the parameters of the system for that condition. The initial disturbance or initial condition is similarly defined. Optimal function for the control is defined via a cost functional. The transition from an initial steady state disturbance to the final steady state is optimal as defined by the cost functional which reflects the constraints mentioned above.

Mathematically, this can be formulated in the following way. We determine control functions u_1 and u_2 (that is, heart rate variation $\dot{H}$ and variation of ventilation rate $\ddot{V}_A$) such that the cost functional

$$\int_0^\infty \Big(q_{as}(P_{as}(t) - P_{as}^f)^2 + q_c(P_{a_{CO_2}}(t) - P_{a_{CO_2}}^f)^2 + q_o(P_{a_{O_2}}(t) - P_{a_{O_2}}^f)^2 + q_1 u_1(t)^2 + q_2 u_2(t)^2 \Big)\, dt \tag{20}$$

is minimized under the restriction of the model system

$$\dot{x}(t) = g(x(t)) + B\,u(t), \qquad x(0) = x^i. \tag{21}$$

The positive scalar coefficients q_{as}, q_c, q_o, q_1, and q_2 determine how much weight is attached to each cost component term in the integrand. The superscript "i" refers to the initial state or disturbance and superscript "f" refers to the final equilibrium or steady state of the system. Equation (21) refers to the system equations (1) to (13) which is a nonlinear system of thirteen differential equations with constant coefficients. Here $x(t) \in \mathbb{R}^{13}$ is given by

$$x(t) = (P_{a_{CO_2}}, P_{a_{O_2}}, C_{v_{CO_2}}, C_{v_{O_2}}, P_{as}, P_{vs}, P_{vp}, S_l, S_r, \sigma_l, \sigma_r, H, \dot{V}_A)^T.$$

TABLE 3. Control parameters

Symbol	Meaning	unit
q_{as}	weighting factor of P_{as} in the cost functional	mmHg^{-2}
q_c	weighting factor of $P_{a_{CO_2}}$ in the cost functional	mmHg^{-2}
q_o	weighting factor of $P_{a_{O_2}}$ in the cost functional	mmHg^{-2}
q_1	weighting factor of u_1 in the cost functional	min^4
q_2	weighting factor of u_2 in the cost functional	$\mathrm{min}^4 \cdot \mathrm{l}_{\mathrm{BTPS}}^{-2}$
u_1	control function, $u_1 = \dot{H}$	min^{-2}
u_2	control function, $u_2 = \ddot{V}_A$	$\mathrm{l}_{\mathrm{BTPS}} \cdot \mathrm{min}^{-2}$

$u(t) \in \mathbb{R}^2$ denotes the control vector

$$u(t) = (u_1(t), u_2(t))^T = (\dot{H}, \ddot{V}_A)^T.$$

We linearize the system around the final state x^f defining a linear system of ODE's with initial condition $x(0) = x^i$. Explicitly, we compute a feedback control for the linearized system:

$$u(t) = -F_m\, x(t) \tag{22}$$

where F_m is the feedback gain matrix. The calculated control transfers the linear system from the initial perturbation or state to the final steady state of the system in the optimal way as defined above. This control is optimal for the linearized system around the final steady state x^f and when implemented for the nonlinear system is suboptimal in the sense of Russell [18]. Table 3 refers to the parameters which appear in the cost functional. In the next section, we will apply this concept to the transition from resting awakeness to sleep. We will view the "awake state" as an initial perturbation of the steady state "stage 4 sleep" For a survey of applications of optimal control theory in biomedicine see, e.g., Swan [2] or Noordergraaf and Melbin [19]. For general control theory see Russell [18].

4. **Sleep.** We will now discuss the physiology of sleep and tha approach to modeling sleep.

4.1. **Physiology of sleep.** As one makes the transition between the resting awake state and stage 4 sleep (non dreaming or NREM sleep) a number of physiological changes occur which affect the functioning of the cardiovascular-respiratory control system. The withdrawal of the so-called "wakefulness stimulus" reduces the effective responsiveness of the respiratory chemical control system to levels of CO_2 and O_2 in the blood. One aspect of this reduced responsiveness can be seen in the lower muscle tone during sleep which affects the reaction of the respiratory muscles to control signals. As a consequence, $\dot{V}_A$ falls as one transits to stage 4 sleep. See e.g., Krieger *et al.* [20]. Metabolic rates are also reduced. See, e.g., Batzel and Tran [13] or Khoo *et al.* [21] for further details. The net effect is a decrease in $P_{a_{O_2}}$ and an increase in $P_{a_{CO_2}}$. Furthermore, heart rate and blood pressure fall. Cardiac output generally falls though the degree of decrease is variable and general sympathetic activity is reduced. See, e.g., Somers *et al.* [22] and Shepard [23].

4.2. **Modeling sleep.** The stationary equations for the system (1) to (13) determine a two-degrees of freedom set of steady states. Therefore we need to choose the steady state values of two state variables as parameters. In general we choose values for $P_{a_{CO_2}}$ and H. These quantities are chosen as the parameters for the equilibria because $P_{a_{CO_2}}$ is tightly controlled independently of the special situation and H is easily and reliably measured. In modeling the transition from the "resting awake" steady state to "stage 4 (NREM) sleep" the following steps are carried out:

- We first compute the steady states "resting awake", x^a, and "stage 4 sleep", x^s.
  The steady state "sleep" is defined by such parameter changes as:
  - lower O_2 demand (MR_{O_2}) and lower CO_2 (MR_{CO_2}) production,
  - lower heart rate H,
  - higher $P_{a_{CO_2}}$ concentration in arterial blood.
- We seek control functions u_1 and u_2 which transfer system (21) from the initial steady state "awake", x^a, to the final steady state "sleep", x^s. To do this we consider the linearized system around x^s with initial condition $x(0) = x^a$, and the cost functional

$$\int_0^\infty \Big(q_{as}(P_{as}(t) - P_{as}^s)^2 + q_c(P_{a_{CO_2}}(t) - P_{a_{CO_2}}^s)^2 + q_o(P_{a_{O_2}}(t) - P_{a_{O_2}}^s)^2 + q_1 u_1(t)^2 + q_2 u_2(t)^2 \Big)\, dt. \tag{23}$$

  (Again, superscript "a" and superscript "s" will refer to the steady state values "awake" and "sleep", respectively.) We then compute the control functions u_1 and u_2 such that the cost functional is minimized subject to the linearized system. This is accomplished by solving an associated algebraic matrix-Riccati equation whose solution is used to derive the feedback gain matrix as expressed in Eq. (22). In particular, u_1 and u_2 are given as feedback control functions.

- This control is used to stabilize the nonlinear system (21). This control will be suboptimal in the sense of Russell [18].

In the next section we will present the simulation results based on this approach.

5. **Simulation results.** All calculations use Mathematica 3.0 Tool boxes. In the first simulation we solve the stationary equations by choosing the steady state values of $P_{a_{CO_2}}$ and H as parameters. We assume that heart rate falls from 75 to 68 bpm and that $P_{a_{CO_2}}$ rises to 44 mmHg. The parameters chosen for modeling sleep are listed in Table 4.

TABLE 4. Parameters for modeling sleep

Parameter	Awake	Sleep
H	75.0	68.0
A_{pesk}	131.16	131.16
MR_{CO_2}	0.244	0.208
MR_{O_2}	0.290	0.247
$P_{a_{CO_2}}$	40.0	44.0

The computed steady states for resting awake and stage 4 sleep are listed in Table 5. These values are computed from the model using the chosen parameters from table 4. Parameter tables will always give the chosen parameters used for modeling given conditions such as the awake state or NREM sleep state. Steady state tables give the steady states computed from the model with the chosen parameters. Tables 12 to 14 in the appendix give some comparison values from the literature.

The weights in the cost functional are all set equal to the value one with the exception of q_o, the weighting factor of $P_{a_{O_2}}$, which is set to 0.1. We use different weights for CO_2 and O_2 for the following reasons. First, a deviation of 1 mmHg in $P_{a_{CO_2}}$ is a larger percentage change than a 1 mmHg deviation in $P_{a_{O_2}}$. Second, we consider the control system to have as its primary function the control of the $P_{a_{CO_2}}$ level in these simulations. Indeed, for levels of $P_{a_{O_2}}$ in the range of the awake and sleep states, the adult oxyhemoglobin saturation curve indicates a significant reserve of oxygen and the ventilatory control response to $P_{a_{O_2}}$ is more pronounced only at lower levels of $P_{a_{O_2}}$. This is also expressed in empirical relationships between $P_{a_{O_2}}$, $P_{a_{CO_2}}$, and $\dot{V}_A$ given Wasserman *et al.* [24] or Khoo *et al.* [6] (see also Section 7 below). In regards to the other weights it appears that the system reacts in a more sensitive way to deviations in the other variables than to deviations in $P_{a_{O_2}}$. Because we lack more information, we take the same weight for all variables except $P_{a_{O_2}}$.

A parameter identification analysis would be needed to establish more precise weightings among the cost functional components. Furthermore,

TABLE 5. Steady states

Steady State	Awake	Sleep
H	75.00	68.00
P_{as}	96.89	90.23
P_{ap}	17.26	16.45
P_{vs}	3.726	3.851
P_{vp}	7.313	7.419
$P_{a_{CO_2}}$	40.0	44.0
$P_{a_{O_2}}$	102.46	97.75
$P_{v_{CO_2}}$	47.42	50.96
$P_{v_{O_2}}$	36.36	37.46
Q_l	5.062	4.597
Q_r	5.062	4.597
R_s	18.41	18.79
S_l	72.00	65.28
S_r	5.488	4.976
$\dot{V}_A$	5.264	4.080
$V_{str,l}$	0.06749	0.06760
$V_{str,r}$	0.06749	0.06760

for this simulation, we ignore the transition times needed to reduce the metabolic rates during the transition to stage 4 sleep. Therefore we assume a step change of the metabolic rates.

In terms of the states of the system, the model predicts decreases in P_{as} and $\dot{V}_A$ as experimentally observed in the sleep state (see, e.g., Krieger *et al.* [20], Phillipson and Bowes [25], Podszus [26], Mateika *et al.* [27], or Somers *et al.* [22]). Further, the model predicts a decrease in Q as suggested as a possibility in Shepard [23], Mancia [28], or Schneider *et al.* [29] and contractility falls due to the drop in H in the Bowditch effect. With the metabolic rates given in the tables (respiratory quotient 0.86) $P_{a_{O_2}}$ falls by 4.5 mmHg while, for comparison, a respiratory quotient of 0.82 in the model produces a drop of 7.5 mmHg in $P_{a_{O_2}}$. These values are consistent with data provided in Koo [30] *et al.*, Phillipson [25], and Shepard [23]. The fall in ventilation is a little higher than but consistent with data given in Krieger *et al.* [20], Phillipson and Bowes [25]. and Trinder *et al.* [31].

The above model simulation does not exhibit, as research suggests (cf., eg., Mancia [28], Podszus [26], Bevier *et al.* [32], and Somers *et al.* [22]), that peripheral resistance, as well as, perhaps, stroke volume are reduced during NREM-sleep. These effects are due to changes in the sympathetic nervous system control mechanism during sleep (cf., eg., Somers *et al.* [22]). We consider in the next section this aspect of the cardiovascular system.

6. **Influence of the autonomic nervous system.** We investigate the influence of the autonomic nervous system on resistance and on stroke volume. As mentioned above, research suggests that peripheral resistance and perhaps stroke volume are reduced during NREM-sleep as a result of the reduction of sympathetic nervous system activity (see [22]) in the transition

from quiet awake to NREM sleep. The results obtained in the first simulation (Tables 4 and 5) do not reflect this behavior though contractility is seen to fall as a result of the reduction in H.

It is reasonable to expect that peripheral resistance falls modestly with the reduction in sympathetic activity and while the sympathetic activity reduction should further reduce contractility and induce a reduction in stroke volume there are counter forces which can act to raise stroke volume. For example, the increase in cardiac filling pressure and end diastolic volume resulting from lying down would tend to increase stroke volume. In this model, we will not include the influence of position, but examine model predictions from a reduction in contractility due to decreased sympathetic activity. Model simulation predicts a small drop in stroke volume which may be countered by positional influences. The major influence on the reduction in Q will be as a result of the drop in H.

In the basic model, systemic resistance is only adapted by local control mechanisms. Global sympathetic influence is fixed by the parameter A_{pesk}. The local control does not disappear during sleep but the reduced global sympathetic control activity is likely to trigger a small reduction in the global systemic resistance. We will consider A_{pesk} in relation (19) as a gain factor and reduce it to model the global sympathetic effects countering local effects. A more complete model would include more detail for the two contributing components in R_s, one local, one global. Here A_{pesk} is reduced by 5% (see Tables 6 and 7).

The sympathetic system affects contractility by varying the calcium inflow into the cardiac muscle. In the following simulations, contractility parameters are reduced to model effects of the sympathetic system activity reduction during quiet sleep (see Tables 6 and 7). The Bowditch effect parameters β_l in equation (10) and β_r in equation (11) are reduced by 10% in the NREM-steady state.

The above changes, along with the metabolic rates, are reduced stepwise. While not physiologically correct, these step changes still allow for a qualitative study of the dynamics. In Section 8 we will consider simulations with non step changes in the sleep parameters.

TABLE 6. Parameters values: autonomous effects included

Parameter	Awake	Sleep
A_{pesk}	131.16	124.60
β_l	85.89	77.30
β_r	2.083	1.874
H	75.0	68.0
MR_{CO_2}	0.244	0.208
MR_{O_2}	0.290	0.247
$P_{a_{CO_2}}$	40.0	44.0

TABLE 7. Steady states: autonomous effects included

Steady State	Awake	Sleep
H	75.00	68.00
P_{as}	96.89	82.47
P_{ap}	17.26	16.03
P_{vs}	3.726	4.023
P_{vp}	7.313	7.291
$P_{a_{CO_2}}$	40.0	44.0
$P_{a_{O_2}}$	102.46	97.75
$P_{v_{CO_2}}$	47.42	51.19
$P_{v_{O_2}}$	36.36	36.79
Q_l	5.062	4.450
Q_r	5.062	4.450
R_s	18.41	17.63
S_l	72.00	58.75
S_r	5.488	4.478
$\dot{V}_A$	5.264	4.080
$V_{str,l}$	0.06749	0.06544
$V_{str,r}$	0.06749	0.06544

With these assumptions, the qualitative and quantitative changes in steady state values (Table 7) between "resting awake" and "stage 4 sleep" as derived from the model agree with reported behavior of the cardiovascular system. See, eg., Mancia [28], Podszus [26], Somers *et al.* [22], and Mateika *et al.* [27]. Using these parameter values and steady states, we calculate the controls u_1 and u_2. The simulations in Figures 2–4 illustrate the behavior of the system as it stabilizes around x^s starting from the awake state x^a.

As in the calculations for steady states in the last section, the model predicts decreases in P_{as} and $\dot{V}_A$ as experimentally observed in the sleep state (see, e.g., Krieger *et al.* [20], Phillipson [25], Podszus [26], Somers *et al.* [22], and Mateika *et al.* [27]). As before, the model predicts decreases in Q and contractility. The drop in $P_{a_{O_2}}$ and increase in $P_{a_{CO_2}}$ is consistent with data provided in Koo *et al.* [30], Phillipson [25], and Shepard [23]. The model now reflects a drop in stroke volume and systemic resistance. The model also predicts an increase for P_{vs}. See Tables 13 and 14 in the appendix for a summary of state values for the awake and NREM sleep states.

In terms of the dynamical behavior, the model indicates that $\dot{V}_A$ and $P_{a_{O_2}}$ fall below their final steady states and slowly recover to their final values (see Figure 2) and indicates a transient overshoot in P_{vp} (see Figure 4). These simulations predict a steady reduction in cardiovascular values in the transition to "stage 4 sleep". The model shows qualitatively reasonable behavior in the situations which are considered and simulation dynamics are also quantitatively in the right range. A more precise statement is not possible at the moment because dynamical data obtained by tests for the situations we consider are presently not available. We note that there exists a variety of response combinations for various individuals requiring a

parameter identification (which we will consider in future work) if specific data is to be compared.

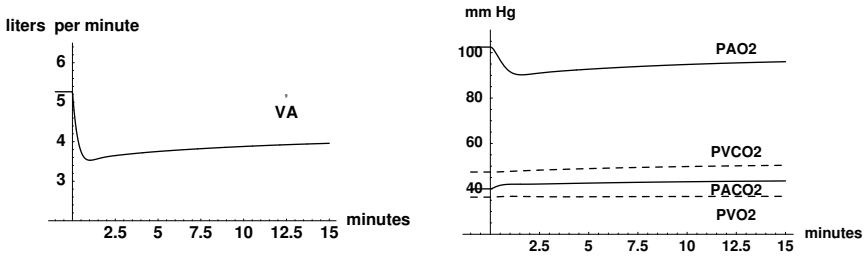

FIGURE 2. Respiratory dynamics

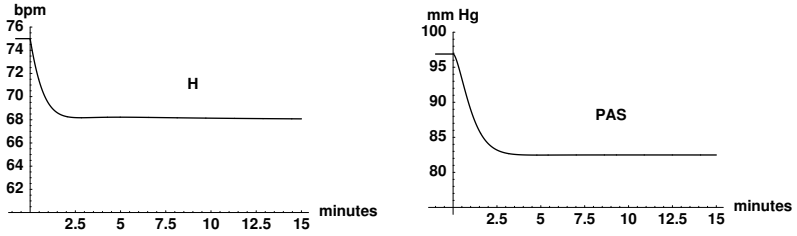

FIGURE 3. Cardiovascular dynamics

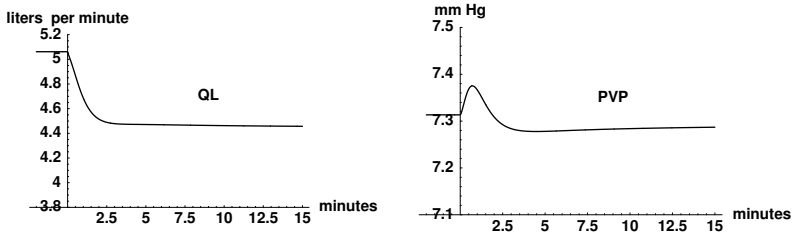

FIGURE 4. Cardiovascular dynamics

For this simulation, as mentioned above, we ignore the transition times needed to reduce the metabolic rates during the transition to "stage 4 sleep". Therefore we assume a step change of the metabolic rates.

Finally, we note that if we assume that the steady state values of cardiac output Q are the same in both the resting awake and NREM-sleep states (using Q as parameter instead of H) then the model predicts nonphysiological behavior as can be seen in Table 8. We have also not changed the parameters β_l and β_r (10) and (11) in this case.

TABLE 8. Steady states: Q assumed fixed

Steady State	Awake	Sleep
Q	5.062	5.062
H	75.03	79.50
P_{as}	96.99	97.32
$P_{v_{O_2}}$	36.42	39.53
R_s	18.43	18.49
S_l	72.03	68.69
$V_{str,l}$	0.06746	0.06367

Note that P_{as} increases in this case by Ohm's law (15) because R_s and Q_l increase. Now, R_s increases because $P_{v_{O_2}}$ increases even though the gain A_{pesk} has been reduced in equation (19). In turn, $P_{v_{O_2}}$ is higher because of the assumed higher value for Q_l in equation 4. Heart rate H increases for the following reasons. Stroke volume $V_{str,l}$ decreases as a result of the increased P_{as} (Frank-Starling's law (18)). To compensate for the decreased stroke volume while maintaining a constant Q_l heart rate must increase in equation (17).

7. **Effects of the Respiratory weights.** Figures 5–6 give the comparisons for $P_{a_{O_2}}$, $P_{a_{CO_2}}$, $\dot{V}_A$, and H for two different weights for $P_{a_{O_2}}$ in the cost functional. The dashed line represents a weight $q_o = 0$ ($P_{a_{O_2}}$ uncontrolled) and the solid line represents q_o= 1 so that the weights of $P_{a_{O_2}}$ and $P_{a_{CO_2}}$ are the same. All other cost functional weights also have value 1. The simulations indicate that the initial drops in $\dot{V}_A$ and $P_{a_{O_2}}$ are much more extreme when $P_{a_{O_2}}$ is not controlled. With equal weights on $P_{a_{O_2}}$ and $P_{a_{CO_2}}$ the initial undershoot of the final steady states is much less pronounced. Simulations indicate that the undershoot is small for q_o greater than 0.3. Experimental data is needed to carry out a parameter identification which would fix the relative weights between the respiratory and cardiovascular cost functional variable groups as well as relative weights within each group. In the above simulations we considered only the relative weights within the respiratory variables.

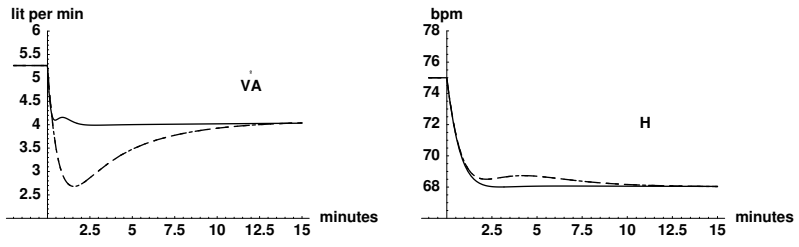

FIGURE 5. Controls compared- dashed: no $P_{a_{O_2}}$ control

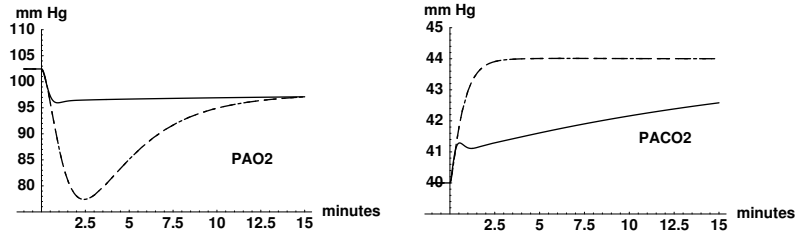

FIGURE 6. Controls compared- dashed: no $P_{a_{O_2}}$ control

As discussed above it is not unreasonable to assign a lower weight to $P_{a_{O_2}}$.

8. **Dynamic comparison of optimal control and an empirical respiratory control.** To further consider these issues and to provide a comparison to the results obtained above we consider as an alternative an empirical control for alveolar ventilation given by Khoo *et al.* [6]. This equation incorporates well known features of the respiratory control system. The control equation is given at steady state as

$$\begin{aligned}\dot{V}_A(t) = G_p \mathrm{e}^{-0.05 P_{a_{O_2}}(t)} \max(0, P_{a_{CO_2}}(t) - I_p) \\ + G_c \max(0, P_{B_{CO_2}}(t) - K - I_c).\end{aligned} \tag{24}$$

In that paper, a relation between $P_{a_{CO_2}}$ and $P_{B_{CO_2}}$ (brain partial pressure of carbon dioxide) was derived and used in the control equation and we use it (as well as a differential equation for $P_{B_{CO_2}}$) in what we refer to as the $\dot{V}_A$ empirical control model. G_p and G_c represent controller gain factors. The symbols I_p and I_c denote cutoff thresholds and the respective ventilation terms become zero when the quantities fall below the thresholds. K is a constant in the steady state relation between $P_{a_{CO_2}}$ and $P_{B_{CO_2}}$. From equation (24) and the parameters given in Table 9 it can be seen that the control consists of two sensory systems which send information on partial pressures of O_2 and CO_2 in the blood to the control processor located in the brain. The first term in equation (24) represents the peripheral sensory center located in the carotid artery in the neck which responds to both $P_{a_{O_2}}$ and $P_{a_{CO_2}}$. The second term in equation (24) represents the central sensory center located in the lower brain which responds essentially to CO_2 levels entering the brain denoted by $P_{B_{CO_2}}$.

The peripheral sensory response to $P_{a_{O_2}}$ and $P_{a_{CO_2}}$ is multiplicative with the contribution by $P_{a_{O_2}}$ becoming more pronounced at lower $P_{a_{O_2}}$ levels. The peripheral response represents a small part (10-25%) of the total ventilatory response at normal blood gas levels.

Dead space effects are incorporated by choosing control gains G_c and G_p at reduced percentage values effectively writing $\dot{V}_A = K_D \cdot V_E$ where $\dot{V}_E$ is minute ventilation. This formulation reduces ventilatory drive by a fixed

percentage and models change in ventilation as change in rate of breathing. See, e.g., Batzel and Tran (2000) [14].

We will now compare the behavior of the optimally derived $\dot{V}_A$ control and the control for $\dot{V}_A$ described by the empirical formula (24). We simulate the case with empirical control for $\dot{V}_A$ given in equation (24) by introducing this formula into the state equations. We remove $P_{a_{O_2}}$, $P_{a_{CO_2}}$, and $\ddot{V}_A$ from the cost functional and the optimal control then represents the control for the cardiovascular system only. Deviations in partial pressures of oxygen and carbon dioxide are compensated for using the empirical formula.

To model the transition to sleep we include an expression given by Khoo *et al.* [33, 21] which incorporates the essential features of the withdrawal of the wakefulness stimulus alluded to in the introduction. This formula for the effect on $\dot{V}_A$ during sleep is given as

$$\dot{V}_{sleep}(t) \quad = \quad G_s(t)(\dot{V}_{awake}(t) - K_{shift}(t)). \tag{25}$$

Note that $\dot{V}_{sleep} = 0$ if $\dot{V}_{awake}(t) \leq K_{shift}(t)$. The time dependencies for G_s and K_{shift} reflect the smooth change in these parameters that occurs in the transition from "awake" state to "stage 4 quiet sleep" state. Once stage 4 sleep is reached these values are constant. $\dot{V}_{awake}$ represents the normal response to blood gas levels which is attenuated during sleep. In general we set the transit time to "stage 4 sleep" to be four minutes. G_s during the awake state is 1 and reduces smoothly to 0.6 at stage 4 sleep. K_{shift} begins at 0 and increases to 5 mmHg by stage 4. The net effect of the transition to stage 4 sleep on the respiratory control response consists in a reduction in the awake gain and a shift in the set point of the controller.

TABLE 9. $\dot{V}_A$ empirical control parameters for modeling sleep

Parameter	Awake	Sleep
G_c	1.44	1.44
G_p	30.24	30.24
G_s	1.0	0.6
K_{shift}	0	4.5
I_C	35.5	35.5
I_P	35.5	35.5
H	75.0	68.0
MR_{CO_2}	0.244	0.208
MR_{O_2}	0.290	0.247
S 4 transit	-	4 min

The parameter values for these equations are given in Table 9. For the transition simulations we assume a 4 minute transition to stage 4 sleep. We will model the time dependent changes by expressions incorporating exponential functions which decrease smoothly in the transition between awake and stage 4 sleep. By adjusting the parameters in these expressions

one can simulate an essentially linear decrease over the entire transition from stage 1 to stage 4 or bias the decrease to the early stages of sleep.

The reduction in sleep gain factor G_s during the transition to stage 4 sleep is modeled by an exponential function which acts essentially linearly between the awake stage and stage 4. The shift in the operating point K_{shift} is reduced in a similar manner with most shift attained by the end of stage 1 sleep (approximately one fourth of the total transition time). We also simulate a decrease in the metabolic rates which is mostly completed by the transition time to stage 2 sleep and also assume the same time dependent decrease for the changes in contractility and systemic resistance. Of course, now the system becomes nonautonomous.

For comparison, we now simulate the case with optimal cardiovascular and optimal respiratory control presented in Section 6 with the same time dependent sleep parameter decrease for metabolic rates and sympathetic effects. Though the system is now nonautonomous, we still implement the control functions u_1 and u_2 calculated for a time-independent linear system around the final steady state "stage 4 sleep". This further reduces the optimality but the thereby obtained (suboptimal) control still stabilizes the system and is useful for dynamic studies.

Figures 7–10 give the comparisons for $P_{a_{O_2}}$, $P_{a_{CO_2}}$, $\dot{V}_A$ and H. The weights in the cost functional are those used in the first simulations.

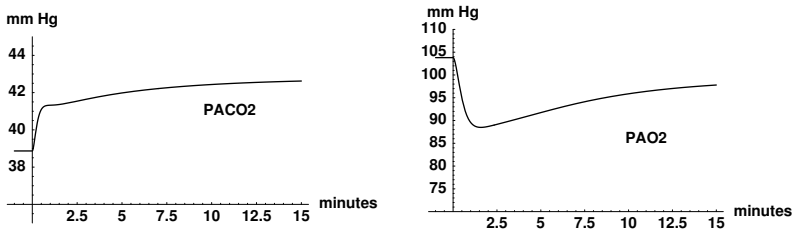

FIGURE 7. Respiratory dynamics: $\dot{V}_A$ empirical control

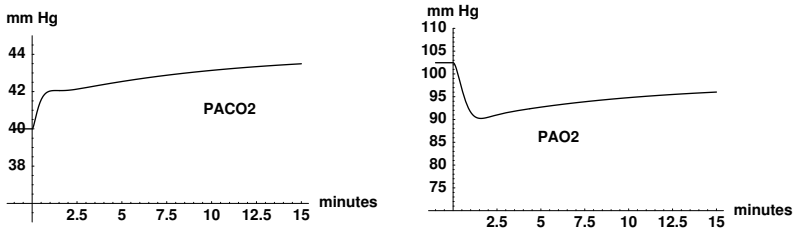

FIGURE 8. Respiratory dynamics: optimal control

As can be seen from the simulations, the two control models act essentially the same. Figures 9–10 give the corresponding control responses to

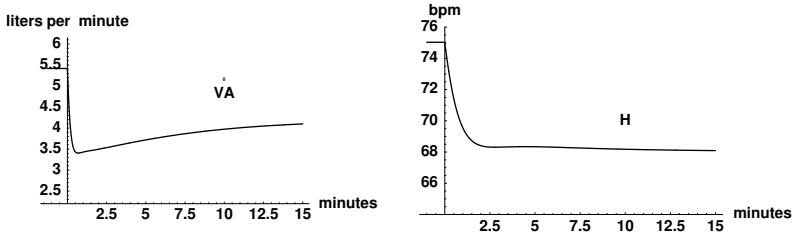

FIGURE 9. Control dynamics: $\dot{V}_A$ empirical control

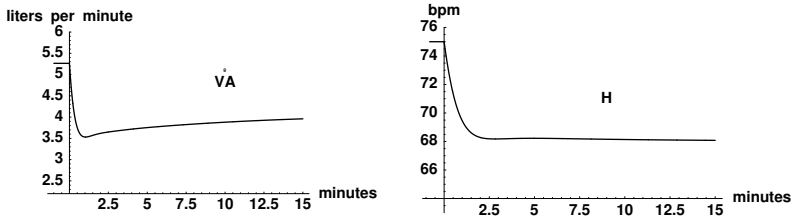

FIGURE 10. Control dynamics: optimal control

the sleep state. The empirical control for $\dot{V}_A$ undershoots with the same qualitative undershoot behavior as exhibited by the optimal model. The overall dynamics for H do not change significantly between the two models even though the respiratory variables are taken out of the cost functional in the $\dot{V}_A$ empirical case. Figures 11 to 14 give the transients of the other important state variables as simulated by the optimal control model.

With this modeling approach, it is possible to explore various parameter effects on the change in time courses. Some reference data can be found in Burgess *et al.* [34] and Trinder *et al.* [31]. Note that there is a continual smooth decline in $V_{str,l}$ and Q, unaffected by EEG sleep stage, while the behavior for H is different in that the largest part of the decline occurred during the initial stage of sleep onset. This behavior for H is consistent with the results in Burgess *et al.* [34] whose data suggests the same disproportionate drop in H during the initial phase of sleep onset or after arousal. The smooth drop in Q and V_{str} is consistent with Bevier *et al.* [32] though that study suggests this smooth drop occurs through the night. Further research is needed to sort out the influences on Q during sleep, including sympathetic effects.

9. **Interaction of the cardiovascular and respiratory weights in the cost functional.** The heart rate simulations indicate that the respiratory and cardiovascular terms in the cost functional do not interact to a significant degree. To explore this issue we vary the weights in the cost functional for the case where both $\dot{V}_A$ and H are given by optimal control.

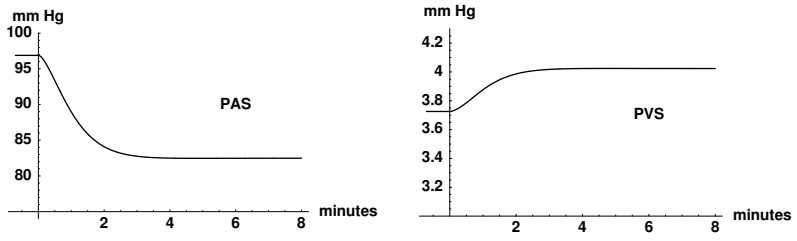

FIGURE 11. Control dynamics: optimal control

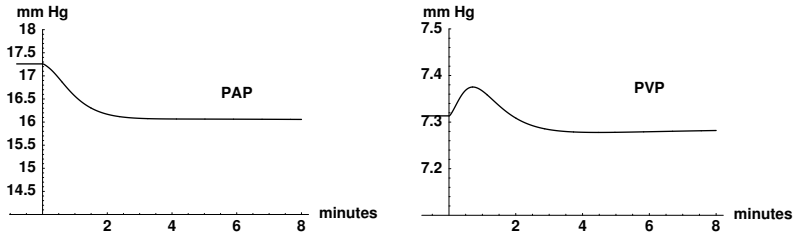

FIGURE 12. Control dynamics: optimal control

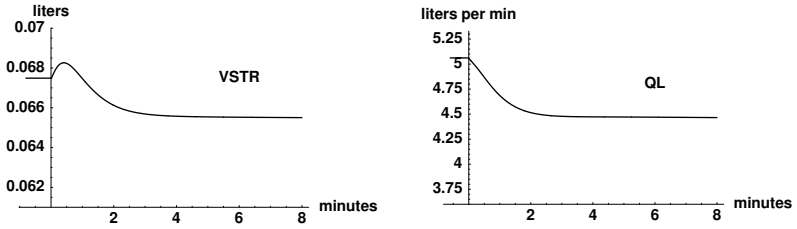

FIGURE 13. Control dynamics: optimal control

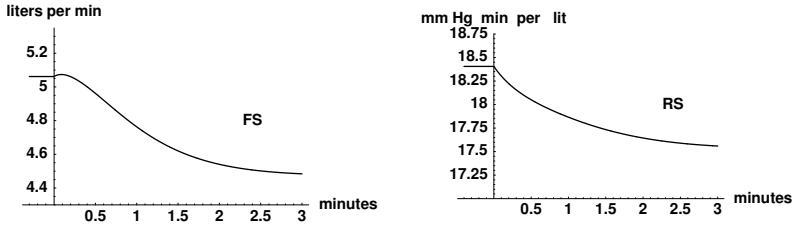

FIGURE 14. Control dynamics: optimal control

Starting from the normal weight distribution, if we take P_{as} as the primary controlled variable and set the weights of the blood gases in the cost functional equal to $q_c = q_o = 0.01$, we get time courses as depicted by the

dashed lines of Figures 15 and 16. On the other hand, if we set the weight of P_{as} equal to $q_{as} = 0.01$ with the respiratory blood gas weights normal thereby making the blood gases the primary controlled variables, then we derive time courses as shown by the dotted lines. The solid lines correspond to the (already discussed) case where P_{as} as well as $P_{a_{CO_2}}$ and $P_{a_{O_2}}$ are normally controlled variables ($q_c = q_{as} = 1$, $q_o = 0.1$). The figures for P_{as} and H indicate that the near absence of the blood gases in the cost functional has little influence on the dynamics of P_{as} and H. Indeed, the dashed and solid lines of P_{as} overlap. A symmetrical situation holds for the blood gases when they are either the primary controlled values or normally controlled as can be seen in solid and dotted line overlap in the figure for $P_{a_{CO_2}}$. In the figure for ventilation rate we do see some interaction in the initial phase of the time course. As more interconnections between the two subsystems are included we would expect that more interaction will occur.

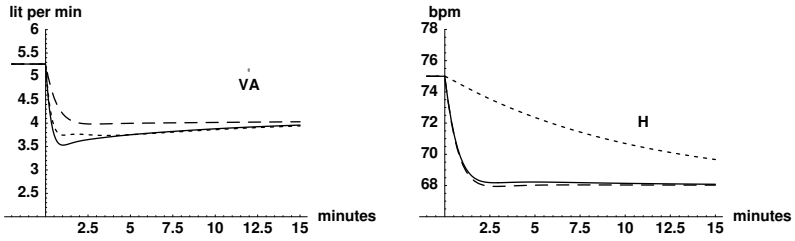

FIGURE 15. Influence of the weights

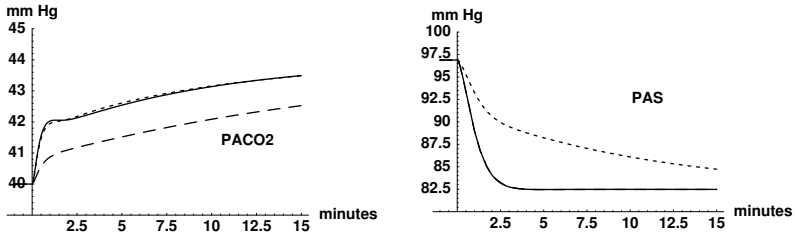

FIGURE 16. Influence of the weights

10. **Conclusion.** In this paper we have considered the adaptation of a cardiovascular-respiratory model developed earlier by Timischl [3] and applied it to the transition from the awake to stage 4 NREM sleep in humans. In the earlier work the model was used to study the transition from rest to non-aerobic exercise with satisfactory results. The current study shows that the model also provides satisfactory predictions for the sleep case. This indicates that the model has the flexibility to study various physiological situations.

In the discussion the model was used to investigate the interplay of the various control variables. A parameter identification would allow for a fuller analysis of these effects. We have compared the dynamics predicted by the optimal control approach with the dynamics of a model incorporating an $\dot{V}_A$ empirical respiratory control. The time courses of the two models were similar.

Acknowledgements. Supported by FWF (Austria) under grant F310 as a subproject of the Special Research Center F003 "Optimization and Control", Institute of Mathematics, University of Graz.

REFERENCES

[1] T. Kenner, Physical and mathematical modeling in cardiovascular systems, in: N. H. C. Hwang, E. R. Gross, D. J. Patel (Eds.), Clinical and Research Applications of Engineering Principles, University Park Press, Baltimore, 1979.

[2] G. W. Swan, Applications of optimal control theory in biomedicine, Marcel Dekker, New York, 1984.

[3] S. Timischl, A global model of the cardiovascular and respiratory system, Ph.D. thesis, Karl Franzens Universität Graz, Austria (1998).

[4] L. B. Rowell, Human Cardiovascular Control, Oxford University Press, New York, 1993.

[5] D. W. Richardson, A. J. Wasserman, J. L. Patterson Jr., General and regional circulatory responses to change in blood pH and carbon dioxide tension, J Clin Invest 40 (1961) 31–43.

[6] M. C. K. Khoo, R. E. Kronauer, K. P. Strohl, A. S. Slutsky, Factors inducing periodic breathing in humans: a general model, J Appl Physiol 53 (3) (1982) 644–59.

[7] F. S. Grodins, J. Buell, A. J. Bart, Mathematical analysis and digital simulation of the respiratory control system, J Appl Physiol 22 (2) (1967) 260–76.

[8] F. S. Grodins, Integrative cardiovascular physiology: a mathematical model synthesis of cardiac and blood vessel hemodynamics, Quart Rev Biol 34 (2) (1959) 93–116.

[9] F. S. Grodins, Control Theory and Biological Systems, Columbia University Press, New York, 1963.

[10] F. Kappel, R. O. Peer, A mathematical model for fundamental regulation processes in the cardiovascular system, J Math Biol 31 (6) (1993) 611–31.

[11] F. Kappel, S. Lafer, R. O. Peer, A model for the cardiovascular system under an ergometric workload, Surv Math Ind 7 (1997) 239–50.

[12] R. Peer, Mathematische Modellierung von grundlegenden Regelungsvorgaengen im Herzkreislauf System, Tech. rep., Technische Universität Graz (1989).

[13] J. J. Batzel, H. T. Tran, Modeling Instability in the Control System for Human Respiration: applications to infant non-rem sleep, Appl Math Comput 110 (2000) 1–51.

[14] J. J. Batzel, H. T. Tran, Stability of the human respiratory control system; part II: analysis of a three dimensional delay state-space model, J Math Biol 41 (1) (2000) 80–102.

[15] F. Kappel, R. O. Peer, Implementation of a cardiovascular model and algorithms for parameter identification, Tech. Rep. 26, SFB Optimierung und Kontrolle, Karl-Franzens-Universität Graz (1995).

[16] C. S. Peskin, Lectures on mathematical aspects of physiology, in: F. C. Hoppensteadt (Ed.), Mathematical Aspects of Physiology, Vol. 19 of Lect Appl Math, Am Math Soc, Providence, Rhode Island, 1981, pp. 1–107.
[17] L. L. Huntsman, A. Noordergraaf, E. O. Attinger, Metabolic autoregulation of blood flow in skeletal muscle: a model, in: J. Baan, A. Noordergraaf, J. Raines (Eds.), Cardiovascular System Dynamics, MIT Press, Cambridge, 1978.
[18] D. L. Russell, Mathematics of finite-dimensional control systems: theory and design, Marcel Dekker, New York, 1979.
[19] A. Noordergraaf, J. Melbin, Introducing the pump equation, in: T. Kenner, R. Busse, H. Hinghofer-Szalkay (Eds.), Cardiovascular System Dynamics: Models and Measurements, Plenum Press, New York, 1982.
[20] J. Krieger, N. Maglasiu, E. Sforza, D. Kurtz, Breathing during Sleep in normal middle age subjects, Sleep 13 (2) (1990) 143–54.
[21] M. C. K. Khoo, A. Gottschalk, A. I. Pack, Sleep-induced periodic breathing and apnea: a theoretical study, J Appl Physiol 70 (5) (1991) 2014–24.
[22] V. K. Somers, M. E. Dyken, A. L. Mark, F. M. Abboud, Sympathetic-nerve activity during sleep in normal subjects, New Engl J Med 328 (5) (1993) 303–7.
[23] J. W. Shepard Jr., Gas exchange and hemodynamics during sleep, Med Clin North Am 69 (6) (1985) 1243–64.
[24] K. Wasserman, B. J. Whipp, R. Casaburi, Respiratory control during exercise, in: A. P. Fishman, N. S. Cherniack, J. G. Widdicombe, S. R. Geiger (Eds.), Handbook of Physiology, Section 3: The Respiratory System, Vol. Volume II, Control of Breathing, Part 2, Am Phys Soc, Bethesda, Maryland, 1986.
[25] E. A. Phillipson, G. Bowes, Control of breathing during sleep, in: A. P. Fishman, N. S. Cherniack, J. G. Widdicombe, S. R. Geiger (Eds.), Handbook of Physiology, Section 3: The Respiratory System, Vol. II, Control of Breathing, Part 2, Am. Phys. Soc., Bethesda, Maryland, 1986.
[26] T. Podszus, Kreislauf und Schlaf, in: H. Schulz (Ed.), Kompendium Schlafmedizin für Ausbildung, Klinik und Praxis, Deutsche Gesllschaft für Schlafforschung und Schlafmedizin, Landsberg, Lech: Ecomed-Verl.-Ges., 1997.
[27] J. H. Mateika, S. Mateika, A. S. Slutsky, V. Hoffstein, The effect of snoring on mean arterial blood pressure during non-REM sleep, Am Rev Respir Dis 145 (1) (1992) 141–6.
[28] G. Mancia, Autonomic modulation of the cardiovascular system during sleep, New Engl J Med 328 (5) (1993) 347–49.
[29] H. Schneider, C. D. Schaub, K. A. Andreoni, A. R. Schwartz, P. L. Smith, J. L. Robotham, C. P. O'Donnell, Systemic and pulmonary hemodynamic responses to normal and obstructed breathing during sleep, J Appl Physiol 83 (5) (1997) 1671–80.
[30] K. W. Koo, D. S. Sax, G. L. Snider, Arterial blood gases and pH during sleep in chronic obstructive pulmonary disease, Am J Med 58 (5) (1975) 663–70.
[31] J. Trinder, F. Whitworth, A. Kay, P. Wilkin, Respiratory instability during sleep onset, J Appl Physiol 73 (6) (1992) 2462–9.
[32] W. C. Bevier, D. E. Bunnell, S. M. Horvath, Cardiovascular function during sleep of active older adults and the effects of exercise, Exp Gerontol 22 (5) (1987) 329–37.
[33] M. C. K. Khoo, A model of respiratory variability during non-REM sleep, in: G. D. Swanson, F. S. Grodins, R. L. Hughson (Eds.), Respiratory Control: a modeling perspective, Plenum Press, New York, 1989.
[34] H. J. Burgess, J. Kleiman, J. Trinder, Cardiac activity during sleep onset, Psychophysiology 36(3) 36 (3) (1999) 298–306.
[35] W. F. Fincham, F. T. Tehrani, A mathematical model of the human respiratory system, J Biomed Eng 5 (2) (1983) 125–133.

[36] R. Klinke, S. Silbernagl (Eds.), Lehrbuch der Physiologie, Georg Thieme Verlag, Stuttgart, 1994.

[37] M. C. K. Khoo, Modeling the effect of sleep-state on respiratory stability, in: M. C. K. Khoo (Ed.), Modeling and Parameter Estimation in Respiratory Control, Plenum Press, New York, 1989.

[38] L. Martin, Pulmonary physiology in clinical practice : the essentials for patient care and evaluation, Mosby Press, St Louis, 1997.

[39] A. C. Guyton, Textbook of Medical Physiology, 7th Edition, W. B. Saunders Company, Philadelphia, 1986.

[40] H. Tsuruta, T. Sato, M. Shirataka, N. Ikeda, Mathematical model of the cardiovascular mechanics for diagnostic analysis and treatment of heart failure: part 1 model description and theoretical analysis, Med Biol Eng Comp 32 (1) (1994) 3–11.

APPENDIX

We assume the following:

$$P_{A_{O_2}} = P_{a_{O_2}},$$
$$P_{A_{CO_2}} = P_{a_{CO_2}},$$

$$P_{B_{CO_2}} = P_{Bv_{CO_2}},$$

$$P_{T_{O_2}} = P_{Tv_{O_2}},$$
$$P_{T_{CO_2}} = P_{Tv_{CO_2}},$$

where v = mixed venous blood, T is tissue compartment.

Further we assume:

- The alveoli and pulmonary capillaries are single well-mixed spaces;
- constant temperature, pressure and humidity are maintained in the gas compartment;
- gas exchange is by diffusion; ventilatory dead space is incorporated via the optimal control $\dot{V}_A$ for the optimal case and control gains G_c and G_p for the empirical case (see text);
- the delay in the respiratory controller signal to effector muscles is zero.
- delay in the baroreceptor signal to the controller and from controller to effector muscles is zero.
- transport delays to the respiratory sensors (and other delays) which can be important when significant alterations from normal steady state behavior occurs are not included in these simulations.
- metabolic rates and other parameters are constant in a given state;
- pH effects on dissociation laws and other factors are ignored or incorporated into parameters;
- acid/base buffering, material transfer across the blood brain barrier, and tissue buffering effects are ignored;
- no inter-cardiac shunting occurs;
- intrathoracic pressure is ignored for this average flow model;
- unidirectional non-pulsatile blood flow through the heart is assumed, and, hence, blood flow and blood pressure are to be interpreted as mean values over the length of a pulse;
- fixed blood volume V_0 is assumed.

The parameters for α, β, and γ, as well as the compliances c_{as}, c_{ap}, c_{vs}, c_{vp}, c_l, and c_r are chosen as in the paper by Kappel and Peer [10]. For the S-shaped O_2 dissociation curve which relates blood gas concentrations to partial pressures we will use the relation

$$C_{O_2}(t) = K_1(1 - e^{-K_2 P_{O_2}(t)})^2. \tag{26}$$

This relation was also used by Fincham and Tehrani [35]. Khoo *et al.* [6] assumes a piecewise linear relationship.

For CO_2, considering the narrow working range of P_{CO_2} we assume a linear dependence of C_{CO_2} on P_{CO_2},

$$C_{CO_2}(t) = K_{CO_2} P_{CO_2}(t) + k_{CO_2}. \tag{27}$$

A linear relationship was also used by Khoo *et al.* [6].

Other parameter and steady state values from the literature are given in the following tables. Parameters normally used for simulations are marked with an asterisk.

TABLE 10. Parameter values (awake rest)

Parameter	Value	Unit	Source
G_c	1.440 *	l/(min ·mmHg)	[6]
	3.2	l/(min ·mmHg)	[33]
G_p	30.240 *	l/(min ·mmHg)	[6]
	26.5	l/(min ·mmHg)	[33]
I_c	35.5 *	mmHg	[6, 33]
	45.0	mmHg	[21]
I_p	35.5 *	mmHg	[6, 33]
	38.0	mmHg	[21]
K_1	0.2	l_{STPD}/l	[35]
K_2	0.046	$mmHg^{-1}$	[35]
k_{CO_2}	0.244	l_{STPD}/l	[6]
K_{CO_2}	0.0065 *	$l_{STPD}/(l \cdot mmHg)$	[6]
	0.0057	$l_{STPD}/(l \cdot mmHg)$	[21]
m_B	1400	g	[36], p. 745
$MR_{B_{CO_2}}$	0.042 *	$l_{STPD}/\min$	[33]
	0.031	$l_{STPD}/(\min \cdot kg$ brain tissue)	[21]
	0.050	$l_{STPD}/\min$	[7]
	0.054	$l_{STPD}/\min$	[35]
MR_{CO_2}	0.21	$l_{STPD}/\min$	[21]
	0.235 *	$l_{STPD}/\min$	[33]
	0.200	$l_{STPD}/\min$	[37]
	0.26 *	$l_{STPD}/\min$	[36] p. 239
MR_{O_2}	0.26	$l_{STPD}/\min$	[21]
	0.290 *	$l_{STPD}/\min$	[33]
	0.240	$l_{STPD}/\min$	[37]
	0.31	$l_{STPD}/\min$	[36] p. 239

TABLE 11. Parameter values (awake rest)

Parameter	Value	Unit	Source
$P_{I_{CO_2}}$	0	mmHg	[6, 7]
$P_{I_{O_2}}$	150	mmHg	[6]
P_{atm}	760	mmHg	[6, 7]
R_p	0.965	mmHg $\cdot$ min /l	[36] p. 233
	1.4	mmHg $\cdot$ min /l	[36] p. 144
	1.95 *	mmHg $\cdot$ min /l	[3]
	1.5-3.0	mmHg $\cdot$ min /l	[38]
RQ	0.88	-	[7]
	0.81	-	[6, 33]
	0.84 *	-	[36] p. 239
$V_{A_{O_2}}$	2.5 *	l_{BTPS}	[6]
	3.0	l_{BTPS}	[7]
	0.5	l_{BTPS}	[39], p. 1011
$V_{A_{CO_2}}$	3.2 *	l_{BTPS}	[6]
	3.0	l_{BTPS}	[21, 7]
$V_{T_{CO_2}}$	15	l	[6, 21, 33]
$V_{T_{O_2}}$	6 *	l	[6, 21, 33]
	1.55	l	[39], p. 1011
$V_{B_{CO_2}}$	0.9 *	l	[33]
	1.0	l	[7]
	1.1	l	[35]
$V_{B_{O_2}}$	1.0	l	[7]
	1.1	l	[35]
V_D	0.15	l_{BTPS}	[21], [36] p. 239
$\dot{V}_D$	2.4	l_{BTPS}/ min	[36] p. 239
	2.28	l_{BTPS}/ min	[6]
F_B	0.5	l/(min $\cdot$kg brain tissue)	[21], [36], p. 745
	0.75-0.8 *	l/ min	[7, 35]
	12-15% of Q	l/ min	[4],p. 242

TABLE 12. Nominal steady state values (awake rest)

Quantity	Value	Unit	Source
$C_{a_{CO_2}}$	0.493	l_{STPD}/l	[36], p. 253
$C_{a_{O_2}}$	0.197	l_{STPD}/l	[36], p. 253
$C_{v_{CO_2}}$	0.535	l_{STPD}/l	[36], p. 253
$C_{v_{O_2}}$	0.147	l_{STPD}/l	[36], p. 253
H	70	min^{-1}	[36] p. 144
P_{ap}	12	mmHg	[36] p. 144
	15	mmHg	[40] p. 4
	10-22	mmHg	[38] Chptr. 8
P_{as}	100	mmHg	[36] p. 144
	93	mmHg	[40] p. 4
P_{vp}	5	mmHg	[36] p. 144
	8	mmHg	[40] p. 4
P_{vs}	2-4	mmHg	[36] p. 144
	5	mmHg	[40] p. 4

TABLE 13. Nominal steady state values (awake rest)

Quantity	Value	Unit	Source
$P_{A_{CO_2}}$	40	mmHg	[39],p. 495, [36] p. 239
$P_{A_{O_2}}$	104	mmHg	[39],p. 494
	100	mmHg	[36] p. 239
$P_{a_{CO_2}}$	40	mmHg	[39],p. 495, [36], p. 253
$P_{a_{O_2}}$	95	mmHg	[39],p. 494
	90	mmHg	[36], p. 253
$P_{v_{CO_2}}$	45	mmHg	[39],p. 495
	46	mmHg	[36], p. 253
	40-50	mmHg	[38] Chptr. 8
$P_{v_{O_2}}$	40	mmHg	[39],p. 494, [36], p. 253
	35-40	mmHg	[38] Chptr. 8
$Q_l = Q_r = F_p = F_s$	6	l/ min	[6, 7]
	6.2	l/ min	[36] p. 239
	5	l/ min	[36] p. 144
	4-7	l/ min	[38] Chptr. 8
R_s	20.	mmHg · min /l	[36] p. 144
	11-18	mmHg · min /l	[38] Chptr. 8
$\dot{V}_A$	4.038	l_{BTPS}/ min	[35]
	5.6	l_{BTPS}/ min	[36] p. 239
$\dot{V}_E$	8	l_{BTPS}/ min	[36] p. 239
$V_{str,l}$	0.070	l	[36] p. 144

TABLE 14. Nominal steady state values (NREM sleep)

Quantity	% change	Model Value	Source
$P_{A_{CO_2}}$	↑ 2-8 mmHg	44.0 mmHg	[23]
$P_{A_{O_2}}$	↓ 3-11 mmHg	97.8 mmHg	[23, 30]
$P_{v_{CO_2}}$	↑ 5 %	51.2 mmHg	estimate
$P_{v_{O_2}}$	↑ 1 %	36.8 mmHg	estimate
$\dot{V}_E$	↓ 14-19 %	6 l_{BTPS}/ min	[23, 20]
P_{as}	↓ 5-17 %	82.5 mmHg	[27, 23, 22]
H	↓ 10 %	68 mmHg	[23, 22]
Q	↓ 0 - 10 %	4.45 l/ min	[23, 29]
$\dot{V}_A$	↓ 14-19 %	4.08 l_{BTPS}/ min	[20]
$\dot{M}R_{O_2}$	↓ 15 %	0.247 l_{STPD}/ min	[21]
$\dot{M}R_{CO_2}$	↓ 15 %	0.208 l_{STPD}/ min	[21]
sympathetic activity	↓ significantly	-	[22]
R_s	↓ 5-10 %	17.6 mmHg · min /l	estimate
S_l	↓ 5-15 %	58.8 mmHg	estimate
S_r	↓ 5-15 %	4.48 mmHg	estimate

E-mail address: susanne.teschl@technikum-wien.at, http://www.esi.ac.at/∼susanne/
E-mail address: jerry.batzel@uni-graz.at, www-ang.uni-graz.at/∼batzel
E-mail address: franz.kappel@uni-graz.at, www.uni-graz.at/imawww/kappel/

TABLE 15. Miscellaneous parameters (awake values)

Quantity	Value	Unit	Source
V_0	5.0	l	[10]
A_{pesk}	131.16	$\text{mmHg} \cdot \text{min} \cdot \text{l}^{-1}$	[10]
α_l	89.47	min^{-2}	[10]
α_r	28.46	min^{-2}	[10]
β_l	85.89	$\text{mmHg} \cdot \text{min}^{-1}$	[10]
β_r	2.08	$\text{mmHg} \cdot \text{min}^{-1}$	[10]
γ_l	37.33	min^{-1}	[10]
γ_r	11.88	min^{-1}	[10]
c_{ap}	0.03557	$\text{l} \cdot \text{mmHg}^{-1}$	[10]
c_{as}	0.01002	$\text{l} \cdot \text{mmHg}^{-1}$	[10]
c_{vp}	0.1394	$\text{l} \cdot \text{mmHg}^{-1}$	[10]
c_{vs}	0.643	$\text{l} \cdot \text{mmHg}^{-1}$	[10]
c_l	0.01289	$\text{l} \cdot \text{mmHg}^{-1}$	[10]
c_r	0.06077	$\text{l} \cdot \text{mmHg}^{-1}$	[10]